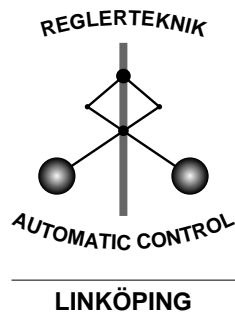# Linear Time-Invariant Models of Non-linear Time-varying Systems

Lennart Ljung

Department of Electrical Engineering
Linköping University, SE-581 83 Linköping, Sweden
WWW: http://www.control.isy.liu.se
Email: ljung@isy.liu.se

October 2, 2001

REGLERTEKNIK

AUTOMATIC CONTROL

LINKÖPING

Estimating Linear Time-Invariant Models of Nonlinear Time-Varying Systems

Lennart Ljung

Div. of Automatic Control

Linköping University

SE-58183 Linköping, Sweden

email: ljung@isy.liu.se

April 10, 2001

Abstract

The standard machinery for system identification of linear time invariant (LTI) models delivers a nominal model and a confidence (uncertainty) region around it, based on (second order moment) residual analysis and covariance estimation. In most cases this gives an uncertainty region that tends to zero as more and more data become available, even if the true system is non-linear and/or time-varying. In this paper, the reasons for this are displayed, and a characterization of the limit LTI model is given under quite general conditions. Various ways are discussed, and tested, to obtain a more realistic limiting model, with uncertainty. These should reflect the distance to the true possibly non-linear, time-varying system, and also form a reliable basis for robust LTI control design.

1 Introduction: The Fiction of an LTI System

Linear, Time-invariant (LTI) descriptions of dynamical systems are clearly the bread and butter of control theory. Nevertheless, they are still a fiction: No real-life system is exactly linear and time-invariant. So, although there are no LTI systems out there, LTI models as a basis for control design have proved to be of enormous value. There are basically two reasons for this: (1) an LTI model may be a good approximation of a real life system and (2) feedback control is forgiving, in the sense that you can achieve good control based on quite an approximate model.

System Identification offers an efficient machinery to estimate LTI models from observed input-output data. This machinery will be briefly surveyed in Section 2. Identification techniques deliver a nominal LTI model, with an associated uncertainty region, reflecting the estimated statistical confidence region of the estimated parameters. It is intuitive to visualize the delivered model as a band around the Nyquist curve or as bands in the Bode plots. These confidence regions are deemed to be reliable (or at least "not falsified") if certain model validation tests are passed. A typical such test is to check the correlation between the model residuals (prediction errors) and past inputs, as well as the correlation among the model residuals themselves.

It is important to realize that the LTI identification machinery is always able to deliver an unfalsified linear model with decreasing uncertainty regions as more and more data become available, regardless of the character of the system. The reason for this is that LTI-techniques (i.e. second order moment techniques) cannot distinguish a system from its LTI second order equivalent. The details of this are discussed in Section 3.

1

Let us illustrate this important fact:

Example 1.1: Rotation of a Rigid Body

Consider the rotation of a rigid body around a fixed point. The input u is a moment applied along a certain axis. The output y is the angular velocity around one of the principal axes of the moment of inertia. If u is applied around the same principal axis, the rotation is decoupled and there is a linear relationship between u and y. However, if u is applied along another axis, the system will not be linear, unless the body is spherically symmetrical. The reason is that there are non-linear cross-couplings between the principal axes of the moment of inertia. To be specific, we consider a thin and long body with moments of inertia being 0.11, 100.01, and 100.10, respectively, along the principal axes. There is also a viscous damping factor of 0.01 around each of the axes. We perform two experiments:

- A. The input moment is applied around an axis that deviates from the output principal axis by 0.003 radians.
- B. The input moment is applied along the line that deviates from the output principal axis by 0.1 radians.

The first system would then be "rather linear", while the second one is highly non-linear.

In each case a low frequency random input was chosen and 10000 data points collected. Portions of the data are shown in Figures 1 - 2. The linear identification process selected a third order BJ model in both cases. Results from residual analysis in the two cases are shown in Figures 3 - 4. Neither give any reason to reject the models. Amplitude Bode plots with confidence regions corresponding to 3 standard deviations are shown in Figures 5 - 6. The delivered picture is clear: Both systems can confidently be described by LTI models with only minor uncertainty.

For experiment A, the model is able to describe 100 % of the output variation by one-step ahead prediction and 99.39 % in a pure simulation. The corresponding figures for experiment B is 99.97 % and 0.13 %, respectively. The last figure is low, but the LTI- identification machinery explains the deviation as noise that is uncorrelated with the input and can be described as filtered white noise disturbances, giving rise to some limited uncertainty in the estimated model.

If we know that the data collection has been essentially noise-free, this interpretation should cause some concern,
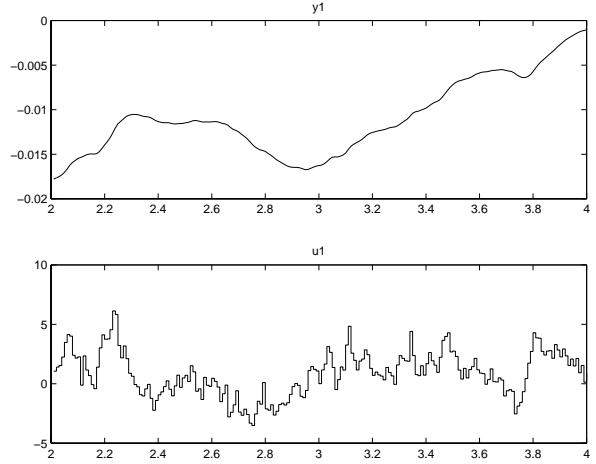

Figure 1: Portions of the data. Experiment A. The upper plot is output (angular velocity around the second principal axis.) and the lower plot is the input (applied moment around another axis.)
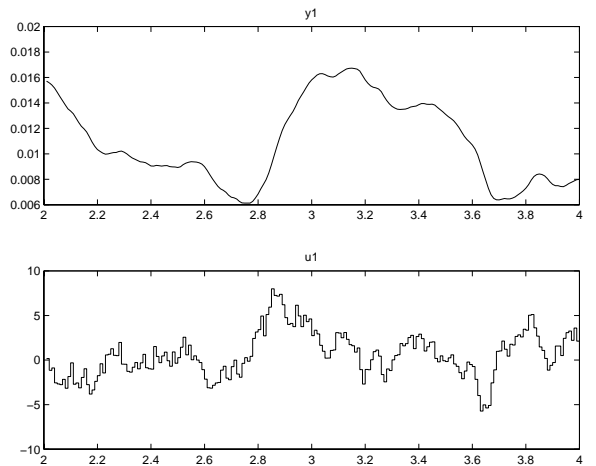

Figure 2: Portions of the data. Experiment B. Output and input as in the previous figure.
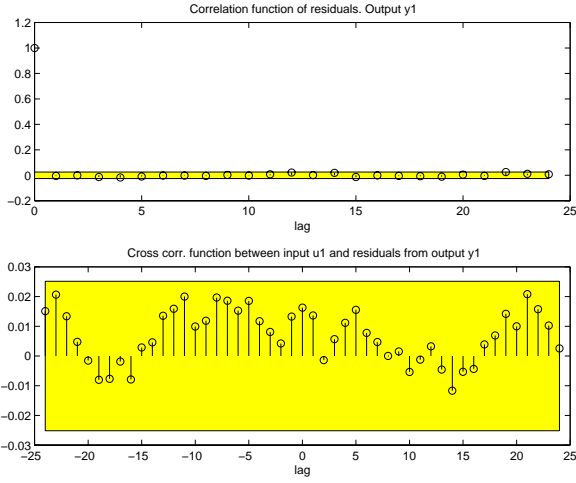
Figure 3: Result of residual analysis. Experiment A. The upper curve shows the autocorrelation of the residuals. The lower plot shows the cross correlation between residuals and inputs. The shaded zone is the confidence region.
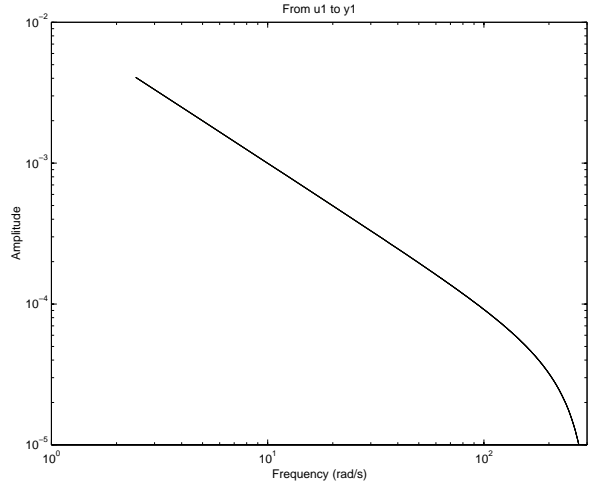

Figure 5: Amplitude Bode plot of the obtained model, with confidence regions corresponding to 3 standard deviations marked. Experiment A.
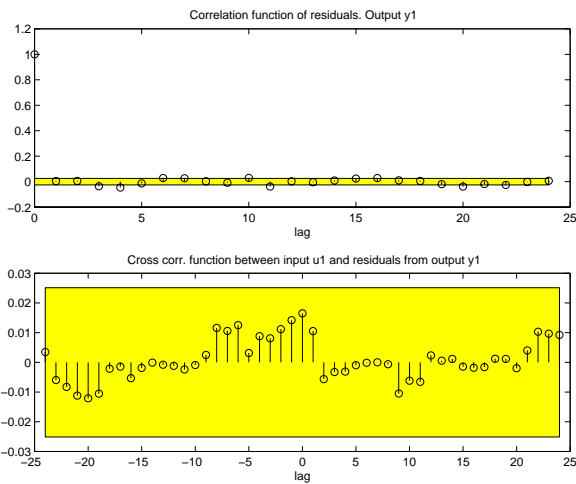

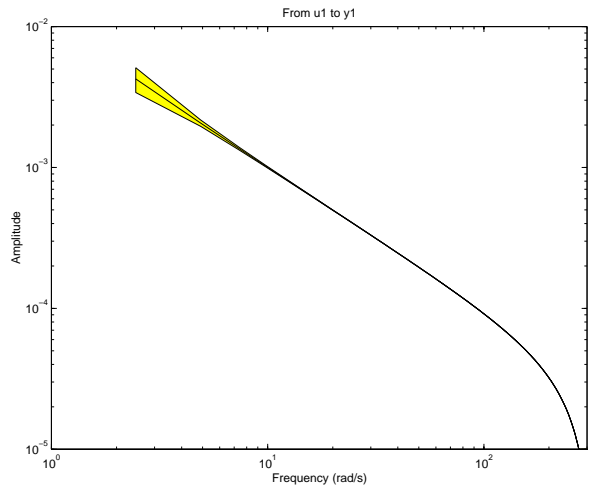Figure 4: Result of residual analysis. Experiment B. Same explanation as in Figure 3.

Figure 6: Amplitude Bode plot of the obtained model, with confidence regions corresponding to 3 standard deviations marked. Experiment B.

but this is the only cloud in the LTI sky. For us, who did the simulation and know that the system in case B is highly non-linear, the Bode plot in Figure 6 and the residual test plot in Figure 4 should call for fundamental concern.

The example points out a fundamental shortcoming of the standard LTI identification process: *With increasing amounts of data, models will be delivered with uncertainty zones converging to zero in Nyquist/Bode diagrams.* This does not rhyme well with our knowledge that while LTI models may be good approximations, no real life system is exactly LTI. It would be much more satisfactory if the delivered LTI model has some remaining uncertainty, no matter how many data it is estimated from.

The topic of this contribution is to discuss this issue.

Dealing with remaining bias errors in models is by no means a new problem. There are many contributions in the literature that deal with the problem to live with both bias errors and the classical statistical variance errors. We could point to, among many references, [1] for a characterization of the bias error in the frequency domain, [2] and [3] for the concept of *stochastic embedding*, [4] for *model error models*, [5] for total error estimates, [6], [7] and [8] for more deterministic measures, [9] for explicit analysis of bias and variance contributions, [10] for model approximations tailored to control design, and [11] for explicit robustness measures for identified models.

Most of these references, however, deal with the problem that the model is of lower order than the true system, which still is assumed to be given as an LTI description. In this paper we will specifically discuss model discrepancies that are caused by systems that are more difficult to describe. An early treatment of LTI models and ill-defined systems is given in Chapter 8 of [12].

2 The Machinery of Estimating LTI Models

A general LTI-model of a dynamical system can always be described as

$$y(t) = G(q, \theta)u(t) + H(q, \theta)e(t) \qquad (1)$$

Here, q is the shift operator, and G and H are the transfer matrices from the measured input u and the noise source e, which is modeled as white noise (sequence of independent random variables). For notational convenience we will from now on only consider Single-Input-Single-Output systems, but the theory is the same in the multivariable case.

We shall also use the following shorthand notation for the corresponding frequency function

$$G_\theta = G(e^{i\omega}, \theta) \qquad (2)$$

The transfer functions are parameterized by a finite-dimensional parameter vector θ, and this parameterization can be quite arbitrary. For black-box models, it is common to parameterize G and H in terms of the coefficients of numerator and denominator polynomials, perhaps constraining G and H to have the same denominators. This leads to well established model classes, known under names like ARX, ARMAX, OE, BJ, etc.

Another possibility is to parameterize the model as a state-space model, in discrete or continuous time:

$$x(t+1) = A(\theta)x(t) + B(\theta)u(t) + K(\theta)e(t) \qquad (3a)$$
$$y(t) = C(\theta)x(t) + D(\theta)u(t) + e(t) \qquad (3b)$$

which gives

$$G(q, \theta) = C(\theta)(qI - A(\theta))^{-1}B(\theta) + D(\theta)$$
$$H(q, \theta) = C(\theta)(qI - A(\theta))^{-1}K(\theta) + I$$

The parameterization of the state-space matrices can be of black-box character as canonical forms, or even filling all the matrices with parameters. It can also be in terms of a grey-box, where physical insight (typically in continuous time descriptions) is used, mixed with parameters with unknown values.

Whatever the parameterization, the problem is to estimate the parameters in (1) based on observed input-output sequences $\{y(t), u(t), t = 1, 2, \ldots, N\}$. Among many suggested algorithms for this, two major approaches are dominating today:

- Sub-space methods

- Prediction error methods

Sub-space methods, e.g. [13], [14], [15], can be described as first estimating the state sequence in (3a) and then treating the two equations, with assumed known x, as linear regressions to find the state space matrices.

Prediction error methods first determine the prediction errors associated with (1):

$$\varepsilon(t, \theta) = H^{-1}(q, \theta)(y(t) - G(q, \theta)u(t)) \qquad (4)$$

This requires θ be confined to a region D, so that the filters H^{-1} and $H^{-1}G$ are stable. Then the θ that minimizes the norm of the errors

$$\hat{\theta}_N = \arg\min_{\theta \in D} V_N(\theta) \qquad (5a)$$

$$V_N(\theta) = \frac{1}{N} \sum_{t=1}^{N} \varepsilon^2(t, \theta) \qquad (5b)$$

is determined, typically by numerical search. A good combination of the two approaches, in the black-box case, is to initialize the search at the estimate provided by the subspace method.

How will these methods perform? Well, that depends on the input-output data. A typical approach to analysis is to assume that the data indeed have been generated by a system like (1) for some particular parameter vector θ_0, and for e being a sequence of independent random variables. In that case the asymptotic statistical properties (convergence and asymptotic distribution) of $\hat{\theta}_N$ can be calculated readily. We refer to [16] for a comprehensive analysis of this kind, as well as for more details on model structures and estimation techniques. Just one thing will be pointed out, though: It is part of the standard LTI-identification machinery to compute the resulting residuals:

$$\varepsilon(t) = \varepsilon(t, \hat{\theta}_N) \qquad (6)$$

It is then tested whether $\varepsilon(t)$ is uncorrelated with past inputs $u(s), s \leq t$ and if they are mutually uncorrelated. If such a *residual analysis test* is passed (i.e. there is no convincing statistical evidence that correlation is present), the assumption of a true system within (1) corresponding to a particular value θ_0 is "not falsified", and the distribution of $\hat{\theta}_N - \theta_0$ can be calculated using the aforementioned theory. This means that a confidence region for the true system can be estimated. The delivered LTI model thus comes with a quality tag, corresponding to confidence regions around the estimate. This was depicted, e.g. in Figure 5.

Instead of reviewing this standard material, we shall in this paper develop an independent analysis of the limit of the prediction error method estimate $\hat{\theta}_N$. This will use minimal assumptions on the properties of the input-output data. In particular, it will not be assumed that they have been generated by an LTI system, and it will not employ a stochastic framework. Some related results were presented in [17].

3 Second Order Equivalent LTI Models

3.1 Quasistationary Signals

A deterministic signal $z(t)$ will be called *quasistationary*, [16], if

$$|z(t)| \leq C, \, \forall t \quad \text{for some } C < \infty \qquad (7a)$$

$$\lim_{N \to \infty} \frac{1}{N} \sum_{t=1}^{N} z(t)z^T(t - \tau) = R_z(\tau), \text{ exists } \forall \tau \qquad (7b)$$

If R_z is such that the Z-transform

$$\Phi_z(z) = \sum_{\tau = -\infty}^{\infty} R_z(\tau)z^{-\tau} \qquad (8)$$

is well defined on the unit circle, we call $\Phi_z(e^{i\omega})$ the *spectrum* or *spectral density* of z. $\Phi_z(z)$ will be called the *spectral function*. It can be shown that R_z and Φ_z possess all the properties normally associated with covariance functions and spectra, defined

for stationary stochastic processes. In Section 4.2 we shall specifically prove how they transform under linear filtering.

We will also use the following standard concepts: A filter

$$G(z) = \sum_{k=-\infty}^{\infty} g_k z^{-k} \qquad (9)$$

will be called

- *stable* if $\sum |g_k| < \infty$

- *causal* if $g_k = 0,\ k < 0$

- *strictly causal* if $g_k = 0,\ k \leq 0$

- *anti-causal* if $g_k = 0,\ k > 0$.

Moreover, a family of filters

$$G_\theta(z) = \sum_{k=-\infty}^{\infty} g_k^\theta z^{-k}, \quad \theta \in D \qquad (10)$$

is called *uniformly stable* if

$$\sum_{k=-\infty}^{\infty} \sup_{\theta \in D} |g_k^\theta| < \infty \qquad (11)$$

3.2 Description of Systems that Produce Quasistationary Data

Let the input-output data collected from the process be $\{u(t), y(t); t = 1, 2, \dots\}$. Let

$$z(t) = \begin{bmatrix} y(t) \\ u(t) \end{bmatrix}$$

Assume that the data are quasistationary and that the spectral function

$$\Phi_z(z) = \begin{bmatrix} \Phi_y(z) & \Phi_{yu}(z) \\ \Phi_{uy}(z) & \Phi_u(z) \end{bmatrix} \qquad (12)$$

is well defined.

Now, do spectral factorization

$$\Phi_z(z) = L(z)L^T(1/z)$$

so that $L(z)$ and $L^{-1}(z)$ are stable and causal 2-by-2 transfer function matrices. Then define

$$P(z) = \begin{bmatrix} \Phi_{yu}(z) & \Phi_y(z) \end{bmatrix} L^T(1/z)^{-1}$$

$$= \sum_{k=-\infty}^{0} p_k z^{-k} + \sum_{k=1}^{\infty} p_k z^{-k} = P_-(z) + P_+(z)$$

where $P_+(z)$ is the strictly causal part of the left hand side. Next define W_u and W_y by

$$P_+(z)L^{-1}(z) = \begin{bmatrix} W_u(z) & W_y(z) \end{bmatrix} \qquad (13)$$

By construction W_u and W_y will be strictly causal, i.e. start with a delay (contain a factor $1/z$). The reader will recognize

$$\hat{y}(t|t-1) = W_u(q)u(t) + W_y(q)y(t) \qquad (14)$$

as the Wiener filter, [18] for estimating (predicting) $y(t)$ from $u(s), y(s); s \leq t - 1$. Let

$$e_0(t) = y(t) - \hat{y}(t|t-1)$$

Then (14) can be rearranged as

$$y(t) = G_0(q)u(t) + H_0(q)e_0(t) \qquad (15a)$$

with

$$H_0(z) = (I - W_y(z))^{-1} \qquad (15b)$$
$$G_0(z) = H_0(z)W_u(z) \qquad (15c)$$

By the properties of the Wiener filter $e_0(t)$ will be uncorrelated with $y(s), u(s), s \leq t - 1$, i.e.

$$\lim_{N \to \infty} \frac{1}{N} \sum_{t=1}^{N} e_0(t) \begin{bmatrix} y(t-\tau) \\ u(t-\tau) \end{bmatrix} = \begin{bmatrix} 0 \\ 0 \end{bmatrix}, \forall \tau \geq 1 \qquad (16)$$

Since $e_0(s)$ is constructed from $y(r), u(r), r \leq s$, this also implies that

$$\lim_{N \to \infty} \frac{1}{N} \sum_{t=1}^{N} e_0(t)e_0(t-\tau) = 0 \text{ for } \tau \neq 0 \qquad (17)$$

The corresponding limit for $\tau = 0$ we denote by λ_0. Let

$$\zeta(t) = \begin{bmatrix} u(t) \\ e_0(t) \end{bmatrix}$$

6

Defining spectra analogously to (7b)-(8) gives

$$\Phi_\zeta(z) = \begin{bmatrix} \Phi_u(z) & \Phi_{ue}(z) \\ \Phi_{eu}(z) & \lambda_0 \end{bmatrix} \qquad (18)$$

where $\Phi_{ue}(z)$ will be an anti-causal function, in view of (16).

Remark. Note that Φ_{ue} will normally not be zero, even if there is no feedback in the data. An explicit example of a non-linear, causal, feedback-free relationship between u and y that still gives a non-zero (but non-causal) correlation between u and e is given in Example 1 of [19]. □.

The point of this discussion is of course that any quasistationary input-output data set
$\{z(t), t = 0, 1, \dots\}$
can be seen as being produced by (15a), with a signal e_0 which has a constant spectrum ("white noise") and such that $e_0(t)$ is uncorrelated with past $u(s), s < t$ (i.e. (16) holds.) Statistical independence between e and u and among e will generally not hold. Anyway, we have not introduced any stochastic framework for the data.

This means that *considering just second order properties (i.e. the spectra) of the signals y and u, we cannot disprove that they have been generated by (15a)*. In other words, *the system (15a) is a* **second order equivalent** *of the system that generated y from u.*

Now, it must immediately be said that G_0 and H_0 will in general depend on the input spectrum Φ_u, so that the second order equivalent obtained for one input may be useless to describe the true system for another input.

4 A Characterization of the Limit Model

We shall in this section develop some results about limits of estimated LTI-models based on data from arbitrary systems. The theory will actually be self-contained and it will not rely upon the traditional convergence results for identified models, given e.g. in [16].

4.1 The Theorem

The result is as follows

Theorem 4.1 *Consider the input-output data $\{u(t), y(t); t = 1, 2, \dots\}$. Assume that the data are quasistationary and that W_u and W_y given by (12) – (13) are well defined and stable. Consider the LTI model structure (1) and let the estimate $\hat{\theta}_N$ be defined by (5a). Then*

$$\lim_{N \to \infty} \hat{\theta}_N$$

$$= \arg\min_\theta \int_{-\pi}^{\pi} \frac{1}{|H_\theta|^2} \left[(G_0 - G_\theta) \quad (H_0 - H_\theta) \right] \times$$

$$\begin{bmatrix} \Phi_u & \Phi_{ue} \\ \Phi_{eu} & \lambda_0 \end{bmatrix} \begin{bmatrix} \overline{(G_0 - G_\theta)} \\ \overline{(H_0 - H_\theta)} \end{bmatrix} d\omega$$

$$(19)$$

Here G_0 and H_0 are defined from u and y by (12) -(15b), the argument $e^{i\omega}$ of all the transfer function has been omitted as in (2), and overbar denotes complex conjugation.

Note that this is exactly the same result that holds w.p.1 in case it is assumed that (15a) has generated the data with e_0 being a sequence on independent random variance with zero mean values and variance $= \lambda_0$. This is the basic, "traditional" convergence result, see e.g. [16]. This means that all traditional analysis of limiting estimates in open and closed loop can be directly applied to the general, non-linear, non-stochastic case dealt with here, since that just amounts to an analysis of the integral in (19). See, for example, [20].

To prove this theorem we first establish a result of independent interest:

4.2 Transformation of Spectra by Linear Systems

Theorem 4.2 *Let $\{w(t)\}$ be a deterministic, quasistationary signal with spectrum $\Phi_w(\omega)$ and let $G(q)$ be a stable filter. Let*

$$s(t) = G(q)w(t) \qquad (20)$$

Then

$$z(t) = \left(\begin{array}{c} s(t) \\ w(t) \end{array} \right)$$

is also quasistationary with spectrum

$$\Phi_z(\omega) = \left(\begin{array}{cc} G(e^{i\omega})\Phi_w(\omega)G^T(e^{-i\omega}) & G(e^{i\omega})\Phi_w(\omega) \\ \Phi_w(\omega)G^T(e^{-i\omega}) & \Phi_w(\omega) \end{array} \right)$$

The proof of this theorem is given in Appendix A. We may note that the results still parallel the theory of stationary stochastic processes. The expressions for transforming spectra are entirely analogous.

For families of linear filters we have the following results.

Theorem 4.3 *Let $\{G_\theta(q), \theta \in D\}$ be a uniformly stable family of linear filters (see (11)) and let $\{w(t)\}$ be a quasistationary sequence. Let*

$$s_\theta(t) = G_\theta(q)w(t)$$

$$R_s(\tau, \theta) = \lim_{N \to \infty} \sum_{t=1}^{N} s_\theta(t)s_\theta^T(t - \tau)$$

Then, for all τ

$$\sup_{\theta \in D} \left|\left| \frac{1}{N} \sum_{t=1}^{N} s_\theta(t)s_\theta^T(t - \tau) - R_s(\tau, \theta) \right|\right| \to 0 \; as \, N \to \infty$$

Proof

We only have to establish that the convergence in (48) (in the appendix) to zero is uniform in $\theta \in D$. In the first step all the $g(k)$ terms carry an index $\theta : g_\theta(k)$. Interpreting

$$g(k) = \sup_{\theta \in D} |g_\theta(k)|$$

(48) will of course still hold. Since the family $G_\theta(g)$ is uniformly stable

$$\sum_{k=0}^{\infty} g(k) < \infty$$

and this was the only property of $\{g(k)\}$ used to establish that (48) tends to zero. This completes the proof.

$\square$

4.3   Proof of Theorem 4.1

The prediction errors according to the model (1) are

$$\varepsilon_\theta = H_\theta^{-1}(y - G_\theta u) \tag{21}$$

where we have suppressed all arguments. The estimate is determined by minimization of

$$\hat{\theta}_N = \arg\min \sum_{t=1}^{N} \varepsilon_\theta^2 \tag{22}$$

Studying the second order properties of ε_θ, we can replace y with its second order equivalent description (15a). Inserting that expression for y in (21) gives

$$\begin{aligned} \varepsilon_\theta &= H_\theta^{-1}(G_0 u - G_\theta u + H_0 e_0) \\ &= H_\theta^{-1}[(G_0 - G_\theta)u + (H_0 - H_\theta)e_0] + e_0 \\ &\stackrel{\triangle}{=} v_\theta(t) + e_0(t) \end{aligned} \tag{23}$$

According to Theorem 4.2 ε, v_θ and e_0 are quasistationary signals, and according to Theorem 4.3

$$\sum_{t=1}^{N} \varepsilon_\theta^2(t) \to \bar{V}(\theta) + \lambda_0 \tag{24}$$

$$\text{uniformly in } \theta \in D \text{ as } N \to \infty \tag{25}$$

$$\text{where } \bar{V}(\theta) = \lim_{N \to \infty} \frac{1}{N} \sum_{t=1}^{N} v_\theta^2(t) \tag{26}$$

where we also used the limits in (16) and (17). With the notation of (7b) $\bar{V}(\theta) = R_{v_\theta}(0)$, so from the inverse Fourier transform (or Parseval's relationship) we have that

$$\bar{V}(\theta) = \int_{-\pi}^{\pi} \Phi_{v_\theta}(e^{i\omega})d\omega \tag{27}$$

where Φ_{v_θ} is the spectrum of v_θ, which according to (23) and Theorem 4.2 is given by

$$\frac{1}{|H_\theta|^2} \left[(G_0 - G_\theta) \quad (H_0 - H_\theta) \right] \times \tag{28}$$

$$\begin{bmatrix} \Phi_u & \Phi_{ue} \\ \Phi_{eu} & \lambda_0 \end{bmatrix} \begin{bmatrix} (\bar{G}_0 - \bar{G}_\theta) \\ (\bar{H}_0 - \bar{H}_\theta) \end{bmatrix} \tag{29}$$

which proves the theorem.

8

5 General Model Error Models

Any estimated model will be an imperfect description of the system. The term *Model Error Model* was coined in [4] to denote any way to characterize the errors associated with the model. These ways will of course themselves be imperfect, but they may be adequate to describe the amount of caution that should be exercised when the nominal model is used. The basic model error model could simply be described by a parallel block to the nominal model is shown in Figure 7.

How do we gain information about the model error model? Well, all information is in the measured data, possibly in conjunction with some data-independent prior knowledge. Since the nominal model has squeezed out most − or part − of the information in the data, the model error model will describe the relationship between the input u and the output error $v(t) = y(t) − G(q, \hat{\theta}_N)u(t)$ or the residuals $\varepsilon(t) = \varepsilon(t, \hat{\theta}_N)$. This is also illustrated in Figure 7. Consequently, developing a model error model amounts to some kind of *residual analysis*. This is a standard topic in regression theory, see e.g. [21], and the analysis of correlation between past inputs and residuals, depicted, e.g. in Figure 3 is the most common example of such analysis.
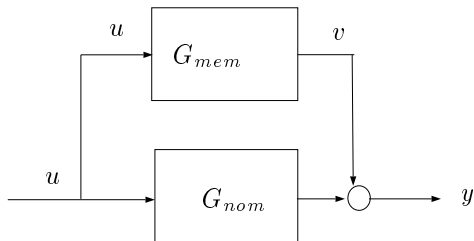

Figure 7: The nominal model G_{nom} and the model error model G_{mem}.

Building linear model error models is thus just an alternative way of phrasing the result of such standard (second order) residual analysis. See [4]. Explicit linear model error models will consequently describe the bias distribution of the nominal model, but will have no information about possible errors due to non-linearities or time-variation in the true system. The nominal model plus the linear model error model will just describe the LTI-equivalent, defined in Section 3.

It is therefore of more interest to discuss error models that are nonlinear and/or time-varying. A brief discussion of this is given in [22]. Now, the purpose of an error model is not to complement the nominal model with detailed structural information. That should rather be done as part of the nominal model. Instead, the purpose of the error model is to capture the reliability of the nominal model, so that proper robustness in the control design can be assured.

This means that we shall work with a model error model depicted in Figure 8. We shall only be concerned about the gain of the block $\tilde{g}_{mem}$. Written out as equations we have
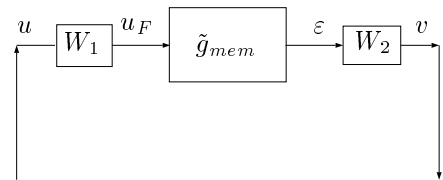

Figure 8: The model error model with linear weighting functions

$$\varepsilon(t) = W_2^{-1}(q)v(t) \tag{30a}$$
$$u_F(t) = W_1(q)u(t) \tag{30b}$$
$$\varepsilon(t) = \tilde{g}_{mem}(u_F^{t-1}) \tag{30c}$$
$$\|\varepsilon\| \leq \beta\|u_F\| + \alpha \tag{30d}$$

Some comments are in order:

- The role of the weighting functions W_1 and W_2 is to give adequate freedom for the control design. Estimating just the gain of the middle block could be an obtuse instrument, and the linear weights will prove useful.

- The norms in (30d) are to be interpreted in L_2 sense. With $\alpha = 0$, the number β is consequently the H_∞ gain of the system $\tilde{g}_{mem}$.

- There are two reasons for the off-set term α:

  1. To allow for external signals to enter the error model, as depicted in Figure 9 (α would then be the norm of w)

  2. To allow for possible very large gains for small amplitude signals, which may not be harmful for "practical stability". This is further elaborated in [23]. For discussions of such an off-set term in connection with stability see also [24] and [25].
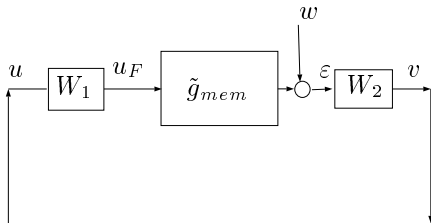

Figure 9: The model error model with additive disturbance

6 Estimating the Gain of a System

We are now faced with an essential problem: *Given the sequences u_F and ε, how to estimate β and α in (30d)?*

There is apparently not an extensive literature on this problem. Some "identification for robust control" articles relate to the gain estimation, like [6], [7], [26], [27], [28] and [29]. These mostly deal with the gain of a LTI or an LTV error model, though.

It is not the purpose of this section to launch a recommended method for gain estimation of general model error models. We shall instead point to some possibilities, that indicate that the problem is not infeasible.

6.1 Estimating the Gain from a Model

A rather obvious possibility is to explicitly estimate the model in (30c) and then compute the gain of the estimated model:

$$\varepsilon(t) = \tilde{g}_{mem}(u_F^{t-1}) + w(t)$$

Use your favorite non-linear black box model structure for $\tilde{g}_{mem}$, such as an Artificial Neural Network, Local Linear Models, Piece-wise linear models, etc. (cf Chapter 5 in [16]). Then determine β and α from the estimated model and the size of w.

As an alternative, if just the gain is of interest, it may be simpler to directly estimate a "ceiling" for the surface that $\tilde{g}_{mem}$ defines. See also Section 6.3.

6.2 Estimating the Gain Directly From Data

It is tempting to circumvent the laborious process of estimating a general nonlinear black-box model and then compute its gain, by directly estimating the gain from the data. For example, if a local, radial basis neural network is used to estimate the surface $\tilde{g}_{mem}$, the "peaks" of this surface are created by large values of observed $\varepsilon(t)$. (See Section 6.3 for more intuition about this "surface.") The highest gain points of the surface are created by observations where the ratio $|\varepsilon|$ to $\|u\|$ is large. This leads to the following simple method:

- Assume that it is known that most of the influence on $\varepsilon(t)$ from past $u_F(s), s \le t$, linear or not, lasts for d samples. Simple transient experiments, or basic prior knowledge can give insight into this. Form

$$\varphi(t) = \begin{bmatrix} u_F(t-1) & u_F(t-2) & \ldots & u_F(t-d) \end{bmatrix} \tag{31a}$$

and find

$$\rho = \max_t \frac{|\varepsilon(t)|}{\|\varphi(t)\|} \tag{31b}$$

Here $\| \cdot \|^2$ is the usual 2-norm. Now, ρ is the largest gain to a single value of ε that we have

seen in the data. To move to a corresponding norm for ε a natural upper bound on the gain would be

$$\hat{\beta} = \sqrt{d} \cdot \rho \qquad (31c)$$

The reason why $\hat{\beta}$ is an upper bound, is that it does not follow that d such large values of ε can be produced in a sequence. Now this is a very simple algorithm, that does not have any provisions for dealing with noise or off-sets. A more general version would be to have an intelligent way of finding a noise-permissive upper-bounding line when regressing $|\varepsilon|$ on $\|\varphi\|$. Here we just let that line go through the origin ($\alpha = 0$) and did not allow any observations above the line.

Anyway, let us test how this estimator works.

Example 6.1: Estimating Gains for Time-Varying, Non-Linear, Noise Corrupted Systems

We create a time-varying, non-linear, noise corrupted system as follows:

- Create two random, linear third order system: `m1=idpoly(fstab([1,randn(1,3)*2],...` `[0,randn(1,3)*3])` and similarly for `m2`.

- Create an input signal u as a white noise normal signal with 1000 samples and low pass filter it by $1/(q - 0.8)$

- Let u pass through a static, discontinuous non-linearity to form u_1:

$$u_1 = \begin{cases} 5u & \text{if } |u| \leq 2 \\ u & \text{else} \end{cases}$$

- Form a time varying linear system from `m1` and `m2` by letting its parameters vary as a cosine with period 200 samples between those of `m1` and `m2`. The output when simulated with u_1 is called y_1.

- Introduce an output dead-zone so that

$$y(t) = \begin{cases} 0 & \text{if } |y_1(t)| \leq 5 \\ y_1(t) & \text{else} \end{cases}$$

- add rectangular distrubuted noise to y so that the signal-to-noise ratio becomes 10 (amplitude-wise)
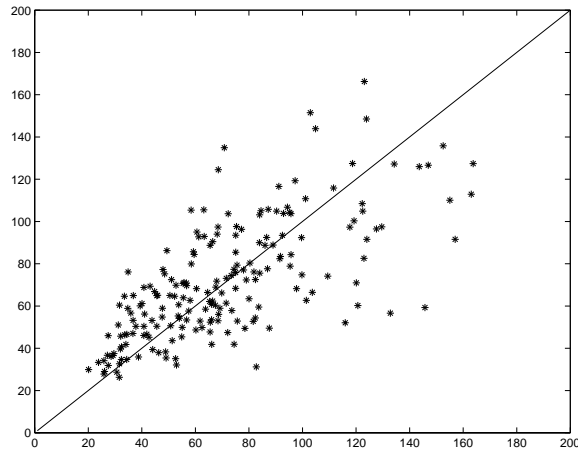

Figure 10: Evaluation of the gain estimator (31). The plot shows the result for 200 simulated systems as described in the text. Each dot corresponds to a system. Its y-coordinate is the estimated gain and its x-coordinate is the true gain.

The theoretical gain of this, non-linear, time-varying system is 5 times the largest magnitude that the frequency functions of `m1` and `m2` ever assume. Two hundred systems of this kind were simulated. Only systems `m1` and `m2` with impulse response solution time (to 5%) less than 20 samples were accepted. The reason is that systems with long impulse responses probably require modified techniques for gain estimation (see Section 6.3).

Figure 10 shows the gain estimate from algorithm (31) versus the true gain. The root mean square deviation of the measure

$$\frac{\text{Estimated Gain}}{\text{True Gain}} - 1 \qquad (32)$$

is 34 %, which could be perceived as a surprisingly good result.

6.3 General Gain Estimates: A Disclaimer

It is instructive to visualize the gain estimation problem as follows: Consider $\mathcal{R}^{d+1}$. Let the "Floor" $\mathcal{R}^d$

11

be spanned by the d-dimensional vectors $\varphi(t)$ and let us view ε as rising perpendicular to this floor. A nonlinear model $\tilde{g}_{mem}$ as in (30c) then is a hypersurface over $\mathcal{R}^d$. Estimating the gain is a matter of finding the highest elevations of this surface as viewed from the origin.

Now, $\mathcal{R}^d$ is a pretty big and "empty" space. Suppose we use $d = 20$ as in the example. Consider the unit cube $|u_F(t)| \leq 1$ and use a grid of fineness 0.2 to distinguish between values of u_F, which is rather crude. Then the unit cube will contain 10^{20} cells. Even with quite a respectable number of observations, like $N = 10^4$, at most a portion of 10^{-16} of the cells will be populated with observations. The surface mentioned above will therefore have an extremely thin support of observations. Finding, and estimating the angle to the peaks of this surface consequently will be a tricky problem. Practically regardless of the number of observations made, most parts of the space have not been covered, and without prior information it is impossible to say what the gain would have been at those parts.

It is in the light of this that the results of Figure 10 could be considered as "surprisingly good".

Now, the longer the effect of an input sample lasts, the more difficult will the gain estimation be, since the probability we will hit the "worst case" input sequence becomes less. This was the reason that we only studied systems with solution time less than 20 samples, which anyway is a reasonably long response time. Systems with longer lasting responses will require modified estimation techniques.

What can be done about this lack of support of observations in $\mathcal{R}^{20}$? Well, essentially nothing. Some possibilities to deal with the problem could be:

1. Obtain more measurements: Will not help much, since $\mathcal{R}^{20}$ would require a totally unrealistic amount of data to be covered.

2. Assume that the surface is "very smooth", and that the collected data exhibit the behavior of the system, that we are likely to encounter also later. This is really the alibi behind algorithm (31).

3. Assume that the surface is a hyperplane, i.e.

that $\tilde{g}_{mem}$ is a linear FIR-model. Or, assume that the actual model surface can be effectively over-bounded by such a hyperplane.

4. Assume that the surface can be well approximated by a radial basis neural network. This is essentially the same as 2.

5. Assume that the surface can be well approximated with a ridge type neural network, such as the traditional sigmoidal networks. This, in a sense, is a combination of 2 and the idea that you can extrapolate along hyperplanes.

It is obvious, in the light of this, that no procedure for estimating the gain can come with any quality guarantees, unless some very reliable prior information is available about the shape of the surface. For a linear error model, it would be possible to describe the distribution of the estimate provided by (31), but in the general case such analytical results cannot be derived.

Estimating the gain in the general case will thus be subject to verification in the particular applications of interest, just as the construction of general nonlinear black-box models.

7 An LTI Model with a General Model Error Model as an Equivalent Uncertain LTI Model

7.1 Linear Model Errors

Once a model with its model error uncertainty is delivered, the question is how to design a controller that will stabilize the system robustly. By this we would mean that the chosen controller should *stabilize all models in the "region" defined by the nominal model and the model error model.*

In case we have used a linear model error model, this region is easily depicted in the frequency domain. It will look like a strip in the Bode, or Nyquist plot, i.e.

$$G \in \mathcal{G} = \{G| \quad |G(e^{i\omega}) - G_{nom}(e^{i\omega})| < \Delta(\omega)\} \quad (33)$$

See, e.g., Figure 5. How to achieve robust stability for such a set of models is well known: Choose a regulator K, such that the complementary sensitivity function

$$T = \frac{G_{nom}K}{1 + G_{nom}K} \qquad (34)$$

is less than the inverse relative model error bound:

$$|T(e^{i\omega})| < \frac{|G_{nom}(e^{i\omega})|}{\Delta(\omega)}, \quad \forall \omega \qquad (35)$$

H_∞ techniques can be used to determine if such a K exists, for given G_{nom} and Δ. See, e.g. [30].

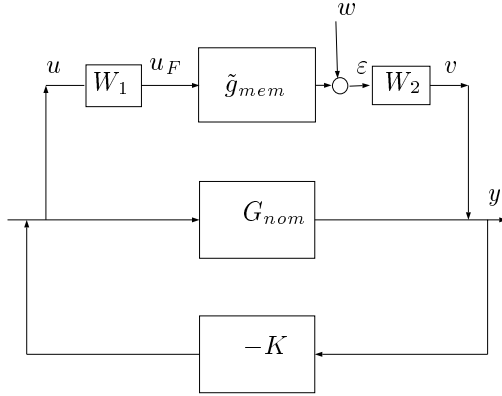## 7.2 Frequency Weighted Non-linear Model Error Model

Figure 11: Block diagram of the feedback loop with model error

The error model (30) corresponds to a closed loop block diagram as in Figure 11. This can be rearranged to be seen as feedback between the non-linear part of the error model $\tilde{g}_{mem}$ and

$$\frac{KW_1W_2}{1 + KG_{nom}}$$

(keeping in mind that we only consider SISO models here). Suppose that the gain of the non-linear part is subject to

$$\|\varepsilon\| \le \beta\|u_F\| + \alpha \qquad (36)$$

as in (30d). Here the off-set term α includes both effects of the non-linearity and of the additive disturbance w. The small gain theorem tells us that stability is assured if

$$\left| \frac{\beta W_1(e^{i\omega})W_2(e^{i\omega})K(e^{i\omega})}{1 + K(e^{i\omega})G_{nom}(e^{i\omega})} \right| < 1 \quad \forall \omega \qquad (37)$$

Comparing with (35) we realize that we just can consider the set of possible system descriptions to be linear and given by

$$G \in \mathcal{G} = \{G| \quad |G(e^{i\omega}) - G_{nom}(e^{i\omega})| < \ldots \qquad (38)$$
$$< \beta W_1(e^{i\omega})W_2(e^{i\omega})\}$$

By stabilizing any linear model in this set, i.e., achieving (35) for $\Delta = \beta W_1 W_2$, we have also made the linear control design robust against non-linear model errors of the type (30).

We can also go beyond stability robustness and consider sensitivity to disturbances. It follows, see [23], that the output norm is bounded by

$$\|y\| \le \|SW_2\|\frac{\alpha}{1 - \beta\|G_w\|}, \quad G_w = T\frac{W_1W_2}{G_{nom}} \qquad (39)$$

where S is the sensitivity and T the complementary sensitivity of the nominal design. Again, standard linear techniques tell us how to design the pair S and T from W_1, W_2, α, β and G_{nom} so that the sensitivity expressed by (39) is acceptable.

7.3 An Equivalent Uncertain Linear Model to be Delivered to the User

From the discussion above it follows that if the LTI identification process estimates a nominal model G_{nom} and we select the weighting functions W_1 and W_2 and then estimate the gain β of the block $\tilde{g}_{mem}$ we can deliver an *LTI uncertainty model* consisting of G_{nom} and the band $\mathcal{G}$ defined by (38). If robust linear control design is applied to this uncertainty model, LTI regulators will be produced that are robust also to non-linear, time-varying model errors up to the size determined by the gain estimator. This extends in a quite natural way LTI-identification + LTI control design to general systems that can be well approximated by LTI models.

13

7.4 Choice of Linear Weights

It may be quite important to correctly use the freedom offered by the weights W_1 and W_2. As will be seen in the next section, different weights can produce quite different LTI uncertainty models. The choice of W is an interplay between shaping the uncertainty regions to what suits the control design, and creating descriptions that leave the unexplained ("β") as small as possible.

Some natural choices are

- $W_1 = G_{nom}$. This makes $u_F = \hat{y}$, the model's simulated output. It is natural to compare the model error with the simulated output, since this directly relates to the percentage of the output's variation that is explained by the model. It also leads to a quantification of the relative model error, which naturally arises in robustness criteria (see e.g. G_w in (39) which contains the ratio W_1/G_{nom}).

- $W_2 = H_{nom}$, the nominal noise model. This makes ε equal to the model residuals, which gives an output the the unknown block with the smallest possible variance. This should lead the the smallest β, but the shape of the uncertainty region may perhaps be unsuitable for control design.

There are of course many other possible choices. One should however avoid weighs with long impulse responses, since this may make the gain estimation more tricky.

8 Some Numerical Experimentation

Let us do some experiments to see how the outlined works out. We first test a time-varying, nonlinear system:

Example 8.1: Estimating LTI models for Non-Linear, Time-Varying Systems

Consider a system that is time-varying between the two descriptions

$$y(t) - 2y(t-1) + 1.45y(t-2) - 0.35y(t-3)$$
$$= u(t-1) + 0.5u(t-2) + 0.2u(t-3)$$

and

$$y(t) - 1.93y(t-1) + 1.43y(t-2) - 0.41y(t-3)$$
$$= 1.05u(t-1) + 0.41u(t-2) + 0.18u(t-3)$$

It is also subject to an input static non-linearity, so that inputs with an amplitude less than 0.8 is multiplied by 1.2, as well as an output dead-zone of length 1. The input is white Gaussian noise with unit variance. A third order LTI model was estimated from the data. This passes the traditional model validations tests well. Figure 12 shows the nominal estimated model and the equivalent uncertain LTI-models, as described in the previous section, with the gain estimated using (31).

Finally, we return to Example 1.1.

Example 8.2: Rotation of a Rigid Body, Cont'd

From the data of experiments A and B (see Figures 1 - 2) nominal third order LTI models were estimated as described in Example 1.1. Error models were estimated as in (30) and (31) for some different W_1 and W_2. Figures 13 and 14 show the amplitude bode plots of the resulting error models. These should be compared with Figures 5 and 6. We see that the essentially linear case of experiment A is correctly identified as such, while the non-linear case of experiment B gives an error model that clearly shows that a reliable linear approximation is not feasible.

---

9 Conclusions

In this contribution four facts have been pointed out:

- Under general conditions we can explicitly specify in which way an estimated LTI model approximates a general system. It is essentially only required that the system produces quasistationary signals.

14

Figure 13: The resulting uncertainty model for Experiment A in Example 1. Left: Relative model error (i.e $W_1 = G_{nom}$) with $W_2 = H_{nom}$. Right: Relative model error with $W_2 = 1$.
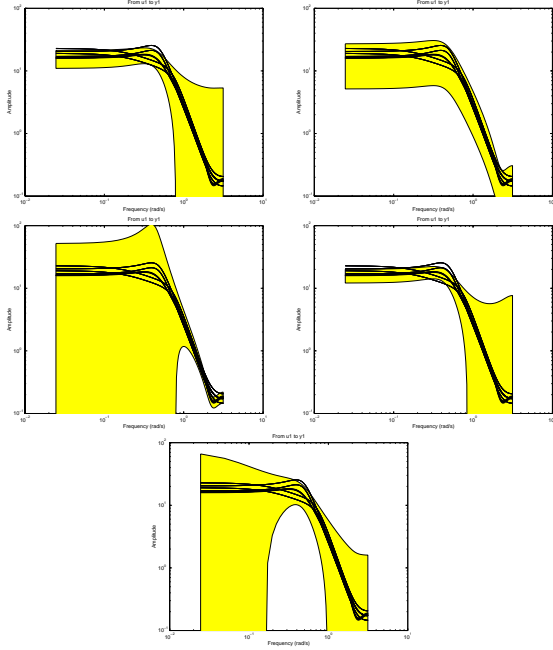
Figure 12: Results from the experiment described in Example 6. The amplitude bode plots show as a light shaded region the error models constructed as in Section 4. The dark shaded region is the nominal estimated LTI model along with an uncertainty region corresponding to 1 standard deviation. The four thin lines are the frequency functions of the two linear systems, each multiplied by 1 and by 1.2 (Recall that there is a static non-linearity with gain between 1 and 1.2.) The plots correspond to different weighting filters W_1 and W_2. From above and left to right:
(1) $W_1 = W_2 = 1$,
(2) $W_1 = G_{nom}$, $W_2 = 1$,
(3) $W_1 = G_{nom}, W_2 = H_{nom}$ (nominal noise model).
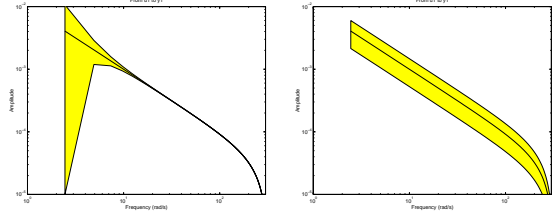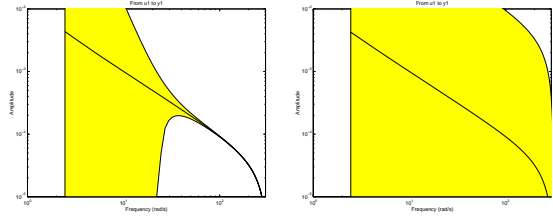(4) $W_1 = 1/(q + 0.3), W_2 = 1$,
(5) $W_1 = 1/(q - 0.95), W_2 = 1$.

Figure 14: The resulting uncertainty model for Experiment B in Example 1. Left: Relative model error (i.e $W_1 = G_{nom}$) with $W_2 = H_{nom}$. Right: Relative model error with $W_2 = 1$.

15

- We have pointed to the possibility of directly estimating the size of the distance between the true system and the LTI-approximation

- We have shown how the resulting model can be seen as an LTI-model with an uncertainty region, much in the same spirit as the traditional model with statistical confidence intervals.

- LTI robust control design for the family of LTI models delivered by this process will give regulators that are robust also to model errors resulting from the possibly nonlinear, time-varying true system

An artifact of the standard LTI identification machinery is that it produces a nominal model with a confidence interval that tends to zero as the number of observed data grows to infinity. This is really an undesired feature, since, realistically, there are no true LTI systems in the real world.

An attractive aspect of the outlined way of delivering uncertain LTI models is that it resembles the classical approach, with the important exception that the uncertainty regions will typically not tend to zero as more and more data become available. There will be some "remaining uncertainty", which should be thought of as a healthy sign.

Now, the outlined process also will need several enhancements:

- More effective gain estimators are required. There should be a good potential for such a development. The fundamental limitation is that you can only base the estimate on what you have seen and typically the observations are but a tiny fraction of the actual response surface. This is more pronounced if the response time to an input change is long. The need to deal with worse signal-to-noise ratios than that in Figure 10 calls for techniques that allow certain observations be outside a bounding cone or a bounding "ceiling" of the response surface. For a time-invariant system this should be quite feasible, but for a time-varying system the distinction between signal and noise is not trivial.

- The error model of Figure 8 could be quite conservative. This is not just a consequence of poor gain estimates, but another reason is that having just a gain measure will not reveal much of the structure of the uncertainty. Put differently, the small gain theorem is quite conservative. It was illustrated in Figure 12 how the uncertainty regions may depend on the chosen weights in an essential way. A more general error model would be to estimate the gain for a block

$$u_F = W_1 u + W_{12} v \quad \text{to} \quad \varepsilon = W_{21} u + W_2^{-1} v \tag{40}$$

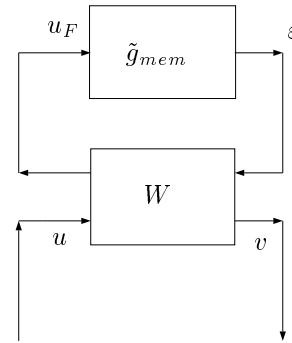This corresponds to an error model as in Figure 15, which is well prepared for LTI control de-

Figure 15: A more general model error model. The 4 transfer functions in the linear block W are rational combinations of the functions W_1, W_2, W_{12}, W_{21} in (40).

sign, using e.g. H_∞ techniques. The case in Figure 9 clearly is the special case $W_{12} = W_{21} = 0$. The two extra weighting functions will give more freedom to customize the error description. At the same time, the resulting LTI uncertainty model (consisting of G_{nom}, the four transfer functions in W and the gain estimate β) is now not simply a band around the Nyquist curve of G_{nom}.

- A third line of thought to pursue, is to move from the symmetric error descriptions inherent in the

gain estimate and the small gain theorem to unsymmetric descriptions, using e.g. IQC's, [31], [32]. While the gain estimate in (31) amounts to finding the scalar β in expressions like

$$\int \begin{bmatrix} \varepsilon(t) & u_F(t) \end{bmatrix} \begin{bmatrix} -1 & 0 \\ 0 & \beta^2 \end{bmatrix} \begin{bmatrix} \varepsilon(t) \\ u_F(t) \end{bmatrix} dt$$
$$\geq 0 \quad \forall u_F, \varepsilon \tag{41}$$

which also can be written in terms of the Fourier transforms of the signals. The more general case (40) corresponds to

$$\int \begin{bmatrix} V(-i\omega) & U(-i\omega) \end{bmatrix} \times$$
$$\begin{bmatrix} \beta^2|W_{12}|^2 - |W_2|^{-2} & \beta^2 W_1\overline{W}_{12} - W_{21}\overline{W_2}^{-1} \\ \beta^2\overline{W_1}W_{12} - \overline{W}_{21}W_2^{-1} & \beta^2|W_1|^2 - |W_{21}|^2 \end{bmatrix}$$
$$\times \begin{bmatrix} V(i\omega) \\ U(i\omega) \end{bmatrix} d\omega \geq 0 \quad \forall u, v \tag{42}$$

The IQC approach would be to find a matrix $\Pi(\omega)$ such that

$$\int \begin{bmatrix} V(-i\omega) & U(-i\omega) \end{bmatrix} \Pi(\omega) \begin{bmatrix} V(i\omega) \\ U(i\omega) \end{bmatrix} dt$$
$$\geq 0 \quad \forall u, v \tag{43}$$

The kinship with the gain estimation is clear from (43), (42). In this case, the delivered LTI uncertainty model would be $\{G_{nom}, \Pi\}$ which may contain more structural information about the character of the uncertainty, related to passivity properties. Control design based on such an uncertainty model is discussed, e.g. in [32].

Appendix A: Proof of Theorem 4.2

Proof

First assume that $w(s) = 0$ for $s \leq 0$ and consider

$$R_s^N(\tau) = \frac{1}{N}\sum_{t=1}^{N} s(t)s^T(t-\tau)$$
$$= \frac{1}{N}\sum_{t=1}^{N}\sum_{k=0}^{t}\sum_{\ell=0}^{t-\tau} g(k)w(t-k)w^T(t-\tau-\ell)g^T(\ell) \tag{44}$$

With the convention that $w(s) = 0$ if $s \notin [0, N]$ we can write

$$R_s^N(\tau) = \sum_{k=0}^{N}\sum_{\ell=0}^{N} g(k)$$
$$\times \frac{1}{N}\sum_{t=1}^{N} w(t-k)w^T(t-\tau-\ell)g^T(\ell) \tag{45}$$

Let

$$R_w^N(\tau) = \frac{1}{N}\sum_{t=1}^{N} w(t)w^T(t-\tau)$$

We see that $R_w^N(\tau+\ell-k)$ and the inner sum in (45) differ by at most $\max(k, |\tau+\ell|)$ summands, each of which are bounded by C according to (7a). Thus

$$|R_w^N(\tau+\ell-k) - \frac{1}{N}\sum^{N} w(t-k)w^T(t-\tau-\ell)|$$
$$\leq C\frac{\max(k, |\tau+\ell|)}{N} \leq \frac{C}{N}(k+|\tau+\ell|) \tag{46}$$

Let us define

$$R_s(\tau) = \sum_{k=0}^{\infty}\sum_{\ell=0}^{\infty} g(k)R_w(\tau+\ell-k)g^T(\ell) \tag{47}$$

Then

$$|R_s(\tau) - R_s^N(\tau)|$$

$$\leq {\sum}' {\sum}' |g(k)||g(\ell)||R_w(\tau + \ell - k)|$$

$$+ \sum_{k=0}^{N} \sum_{\ell=0}^{N} |g(k)||g(\ell)|$$

$$\times |R_w(\tau + \ell - k) - R_w^N(\tau + \ell - k)| \qquad (48)$$

$$+ \frac{C}{N} \sum_{k=0}^{N} k|g(k)| \cdot \sum_{\ell=0}^{N} |g(\ell)|$$

$$+ \frac{C}{N} \sum_{\ell=0}^{N} |\tau + \ell||g(\ell)| \cdot \sum_{k=0}^{N} |g(k)|.$$

Here, the first sum is over the complementary indices of the second one i.e. $k > N$ and/or $\ell > N$. This first sum tends to zero as $N \to \infty$ since $|R_w(\tau)| \leq C$ and $G(q)$ is stable. It follows from the stability of $G(q)$ that

$$\frac{1}{N} \sum_{k=0}^{N} k|g(k)| \to 0 \text{ as } N \to \infty \qquad (49)$$

Hence the last two sums of (48) tend to zero as $N \to \infty$. Consider now the second sum of (48). Select an arbitrary $\varepsilon > 0$ and choose $N = N_\varepsilon$ such that

$$\sum_{k=N_\varepsilon+1}^{\infty} |g(k)| < \varepsilon / [C \cdot C_1] \qquad (50)$$

where

$$C_1 = \sum_{k=0}^{\infty} |g(k)|$$

This is possible since G is stable. Then select N_ε' such that

$$\max_{\substack{1 < \ell < N_\varepsilon \\ 1 < k < N_\varepsilon}} |R_w(\tau + \ell - k) - R_w^N(\tau + \ell - k)| < \varepsilon / C_1^2$$

for $N > N_\varepsilon'$. This is possible since

$$R_w^N(\tau) \to R_w(\tau) \text{ as } N \to \infty \qquad (51)$$

(w is quasistationary) and since only a finite number (which depends on ε) of $R_w(s)$:s are involved (no uniform convergence of (51) is necessary). Then for $N > N_\varepsilon'$ we have that the second sum of (48) is bounded by

$$\sum_{k=0}^{N} \sum_{\ell=0}^{N_\varepsilon} |g(k)||g(\ell)| \cdot \frac{\varepsilon}{C_1^2} + \sum_{k=N_\varepsilon+1}^{\infty} \sum_{\ell=0}^{\infty} |g(k)||g(\ell)| \cdot 2C$$

$$+ \sum_{k=0}^{\infty} \sum_{\ell=N_\varepsilon+1}^{\infty} |g(k)||g(\ell)| \cdot 2C$$

which is less than 5ε according to (50). Hence also the second sum of (48) tends to zero as $N \to \infty$, and we have proved that the limit of (48) is zero, and that hence $s(t)$ is quasistationary.

The proof that $\lim(1/N) \sum_{t=1}^{N} s(t)w(t - \tau)$ exists is analogous and simpler.

For $\Phi_s(\omega)$ we now find that

$$\Phi_s(\omega) = \sum_{\tau=-\infty}^{\infty} \left(\sum_{k=0}^{\infty} \sum_{\ell=0}^{\infty} g(k)R_w(\tau + \ell - k)g^T(\ell) \right) e^{-i\tau\omega}$$

$$= \sum_{\tau=-\infty}^{\infty} \sum_{k=0}^{\infty} g(k)e^{-ik\omega}$$

$$\times \sum_{\ell=0}^{\infty} R_w(\tau - \ell + k)e^{-i(\tau+\ell-k)\omega}g^T(\ell)e^{i\ell\omega}$$

$$= [\tau - \ell + k = s]$$

$$= \sum_{k=0}^{\infty} g(k)e^{-ik\omega} \cdot \sum_{s=-\infty}^{\infty} R_w(s)e^{is\omega} \cdot \sum_{\ell=0}^{\infty} g^T(\ell)e^{i\ell\omega}$$

$$= G(e^{i\omega})\Phi_w(\omega)G^T(e^{-i\omega})$$

Hence the upper left corner of $\Phi_z(\omega)$ is proven. The off diagonal terms are analogous and simpler. $\qquad \square$

References

[1] B. Wahlberg and L. Ljung, "Design variables for bias distribution in transfer function estimation," *IEEE Trans. Automatic Control*, vol. AC-31, pp. 134–144, 1986.

18

[2] B. Ninness and G. C. Goodwin, "Estimation of model quality," *Automatica*, vol. 31, no. 12, pp. 1771–1797, 1995.

[3] G.C. Goodwin, M. Gevers, and B. Ninness, "Quantifying the error in estimated transfer functions with application to model order selection," *IEEE Trans. Automatic Control*, vol. 37, no. 7, pp. 913–929, 1992.

[4] L. Ljung, "Model validation and model error models," in *The Åström Symposium on Control*, B.Wittenmark and A. Rantzer, Eds., pp. 15–42. Studentlitteratur, Lund, Sweden, August 1999.

[5] L. Ljung and L. Guo, "The role of model validation for assessing the size of the unmodeled dynamics," *IEEE Trans. Automatic Control*, vol. AC-42, pp. 1230–1240, 1997.

[6] R. Smith and J. C. Doyle, "Model validation: a connection between robust control and identification," *IEEE Trans. Automatic Control*, vol. AC-37, pp. 942–952, 1992.

[7] R. Smith and G.E. Dullerud, "Continuous-time control model validation using finite experimental data," *IEEE Trans. Automatic Control*, vol. AC-41, pp. 1094–1105, 1996.

[8] R. Kosut, M. K. Lau, and S. P. Boyd, "Set-membership identification of systems with parametric and nonparametric uncertainty," *IEEE Trans. Automatic Control*, vol. AC-37, pp. 929–941, 1992.

[9] R.G. Hakvoort and P.M. van den Hof, "Identification of probabilistic system uncretianty regions by explicit evaluation of bias and variance errors," *IEEE Trans. Autom. Control*, vol. AC-42, no. 11, pp. 1516–1528, Nov 1997.

[10] Michel Gevers, "Towards a joint design of identification and control?," in *Essays on control: Perspectives in the theory and its applications*, H L Trentelman and J C Willems, Eds., ECC '93 Groningen, 1993.

[11] X. Bombois, M. Gevers, and G Scorletti, "A measure of robust stability for an identified set of parameterized transfer functions," *IEEE Trans. Autom. Control*, vol. AC-45, no. 11, pp. 2124–2145, Nov 2000.

[12] Håkan Hjalmarsson, *Aspects in Incomplete Modeling in System Identification*, Ph.D. thesis, Linköping University, Linköping, Sweden, 1993, Linköping Studies in Science and Technology, Dissertations No. 298.

[13] P. Van Overschee and B. DeMoor, *Subspace Identification of Linear Systems: Theory, Implementation, Applications*, Kluwer Academic Publishers, 1996.

[14] M. Verhaegen, "Identification of the deterministic part of MIMO state space models, given in innovations form from input-output data," *Automatica*, vol. 30, no. 1, pp. 61–74, January 1994.

[15] W. E. Larimore, "Canonical variate analysis in identification, filtering and adaptive control," in *Proc. 29th IEEE Conference on Decision and Control*, Honolulu, Hawaii, December 1990, pp. 596–604.

[16] L. Ljung, *System Identification - Theory for the User*, Prentice-Hall, Upper Saddle River, N.J., 2nd edition, 1999.

[17] L. Ljung, "A nonprobabilistic framework for signal spectra," in *Proc. 24th IEEE Conf. on decision and Control*, Fort Laudredale, Fla, 1985, pp. 1056–1060.

[18] Norbert Wiener, *The Extrapolation, Interpolation and Smoothing of Stationary Time Series with Engineering Applications*, Wiley, New York, 1949.

[19] Urban Forssell and Lennart Ljung, "A projection method for closed-loop identification," *IEEE Transactions on Automatic Control*, vol. AC-45, no. 11, pp. 2101 – 2106, Nov 2000.

[20] U. Forssell and L. Ljung, "Closed loop identification revisited," *Automatica*, vol. 35, no. 7, 1999.

[21] N.R. Draper and H. Smith, *Applied Regression Analysis, 2nd ed.*, Wiley, New York, 1981.

[22] Lennart Ljung, "Model error modeling and control design," in *Proc IFAC Symposium SYSID 2000.*, Santa Barbara, CA, Jun 2000, pp. WeAM1–3.

[23] S.T. Glad, A. Helmersson, and L. Ljung, "Robustness guarantees for linar control designs with an estimated nonlinear model error model," in *IEEE Conference on Decision and Control*, Orlando, 2001, Submitted.

[24] V.A. Yakubovich, "Absolute stability of nonlinear control systems in critical cases.," *Avtomatika i Telemekhanika*, vol. 24, no. 3, pp. 293–302, 1963.

[25] M. Vidyasagar, *Nonlinear Systems Analysis*, Prentice-Hall, Englewood Cliffs, NJ, 1993.

[26] R.A. Davis and K. Glover, "An application of recent model validation techniques to flight test data," in *Proc. of the Third European Control Conference ECC95*, Rome, Sept, 1995, pp. 1249 –1254.

[27] R. L. Kosut, "Uncertainty model unfalsification," in *IFAC Symposium on System Identification*, Santa Barbara, CA, 2000.

[28] R. L. Kosut, "Iterative adaptive robust control via uncertainty model unfalsification," in *Proc. 13th IFAC Congress*, San Francisco, July 1996, International federation of Automatic Control, pp. 91–96.

[29] K. Poolla, P. Khargonekar, A. Tikku, J. Krause, and K. Nagpal, "A time domain approach to model validation," *IEEE Trans. Automatic Control*, vol. AC-39, pp. 951–959, 1994.

[30] K. Zhou, J. C. Doyle, and K. Glover, *Robust and Optimal Control*, Prentice-Hall, Englewood Cliffs, NJ, 1996.

[31] V.A. Yakubovich, "The method of matrix inequalities in the theory of stability of nonlinear systems," *Avtomatika i Telemekhanika*, vol. 25, no. 7, pp. 1017–1029, 1964.

[32] A. Megretski and A. Rantzer, "System analysis via integral quadratic constraints," *IEEE Trans. Autom. Control*, vol. AC-42, no. 6, pp. 819–830, June 1997.